



## 3D, anisotropic phase shift operators

Robert J. Ferguson and Gary F. Margrave  
CREWES, University of Calgary

### Summary

Phaseshift operators are presented that enable planewave propagation through media that are transversely anisotropic. These operators propagate planewaves in all three spatial dimensions for all three components, and they are developed to reside at the centre of seismic imaging and modelling by the Rayleigh-Sommerfeld approach. Numerical examples are provided for SV-waves in vertical transverse-isotropy, dipping transverse-isotropy.

### Introduction

Computationally, modelling and imaging conducted in local slowness coordinates hold the promise of high accuracy, high efficiency, plus control of the propagating mode. Seismic wavefields are extrapolated recursively through a geologic model, and reflection and transmission are modelled at each grid level in the model (forward modelling), or an imaging condition is invoked and seismic reflectivity is estimated (imaging). Unlike ray-based approaches, extrapolation raypaths are not restricted to minimum traveltimes (Schneider, 1978) or maximum energy rays (Nichols, 1996) for example, or any other subset of the multi-mode wavefield.

This ability is similar to that of finite-difference approaches (Bording and Lines, 1997), but computation is much more efficient, and control of the propagating mode is always retained - events can be turned on and off if desired without changing the model. Access to this domain is achieved simply through the Fast Fourier transform (Foster and Mosher, 1992; Karl, 1989, pp. 31) so that distribution of data to the nodes of a cluster computer is "embarrassingly parallel" (Foster, 1995, Section 1.4.4 for example). That is, for a single frequency  $\omega$ , the basic unit of data (a matrix) fits easily onto one computational node, and extrapolation, reflection, and transmission experiments proceed on each node independently. At the end of computation (or even during computation if desired), the monochromatic results are gathered and analyzed together.

In the following, we present a set of operators that form the computational inner-loop of seismic imaging and modelling. These operators adapt automatically to dipping interfaces and tilted symmetry angles for transverse isotropy, and they do so for homogeneous 3D media. Solutions for P-waves, SV-waves, and SH-waves are presented, and a number of 3D impulse responses for dipping, fractured media are given as a demonstration.

### Theory

For constant frequency  $\omega$ , ray parameters  $\vec{p} = p_1 \hat{i} + p_2 \hat{j} + p_3 \hat{k}$  define a plane wave in  $\vec{x} = x_1 \hat{i} + x_2 \hat{j} + x_3 \hat{k}$ . Unit vectors  $\hat{i}, \hat{j}$ , and  $\hat{k}$  define the orthogonal coordinate system of the model space. From the scalar wave-equation,  $p_1, p_2$ , and  $p_3$  are coupled according to

$$p_3 = 1/v \sqrt{(1 - (v p_1)^2 - (v p_2)^2)}, \quad (1)$$

where  $v$  is acoustic velocity. Unit normal  $\hat{p}$  to the incident plane-wave is:

$$\hat{p} = \frac{(p_1 \hat{i} + p_2 \hat{j} + p_3 \hat{k})}{\sqrt{(p_1^2 + p_2^2 + p_3^2)}}. \quad (2)$$

For numerical wave-propagation in the Fourier domain  $(k_1, k_2, \omega)$ , where  $k_1$  and  $k_2$  are the Fourier duals of  $x_1, x_2$ , and  $\omega$  is temporal frequency, the normal  $\hat{p}$  to any component of the wave spectrum is available using equation 2. To see this, recall the simple relationships between slowness and wavenumber:  $p_1 = k_1/\omega$  and  $p_2 = k_2/\omega$  plus equation 1 - for any planewave  $\varphi(k_1, k_2, \omega)$ , then,  $\hat{p}$  is defined through equation 2.

The importance of  $\hat{p}$  for a plane wave can be seen in its application to angle-dependent effects like anisotropy with a defined axis of symmetry. For example, for a TTI medium, dip  $\theta$  and azimuth  $\phi$  define the orientation of the azimuthal symmetry axis, and unit normal  $\hat{a}$  associated with the TTI symmetry plane is computed

$$\hat{a} = \sin(\theta) \cos(\phi) \hat{i} + \sin(\theta) \sin(\phi) \hat{j} + \cos(\theta) \hat{k}, \quad (3)$$

and the effective ray-parameter  $p_i$  between  $\hat{p}$  and  $\hat{a}$

$$p_i = \frac{(\sin(\theta_i))}{v} = |\hat{p} \times \hat{a}| \sqrt{(p_1^2 + p_2^2 + p_3^2)}, \quad (4)$$

where  $\theta_i$  and  $p_3$  are evaluated in the incident medium. The form of the left-hand side of equation 4 is convenient for incident media that are also anisotropic. Angle  $\theta_i$  between  $\hat{a}$  and  $\hat{p}$  corresponds to the effective rayparameter  $p_i$  according to equation 4. In the notation of Thomsen (1986), and following Kennett (1983, pp. 236 – 237) and Udias (1990, pp. 268), P- and SV-wave in TI media are given by

$$q_\alpha = \frac{1}{2} \sqrt{\left(\frac{2}{\beta_0^2} + \frac{2}{\alpha_0^2} - 4S p_i^2 - 4R\right)}, \quad (5)$$

and

$$q_\beta^{SV} = \frac{1}{2} \sqrt{\left(\frac{2}{\beta_0^2} + \frac{2}{\alpha_0^2} + 4S p_i^2 - 4R\right)}, \quad (6)$$

respectively, where  $S \Leftrightarrow S(\alpha_0, \beta_0, \varepsilon, \delta)$  and  $R \Leftrightarrow R(P_i, S, \alpha_0, \beta_0, \varepsilon)$  (Ferguson and Sen, 2004). SH-wave velocity is given by

$$q_\beta^{SH} = \sqrt{\left(\frac{1}{\beta^2} - p_i^2 [2\gamma + 1]\right)}. \quad (7)$$

Elastic parameters  $\varepsilon, \delta, \gamma$  and slow-direction velocities  $\alpha_0, \beta_0$  are unique for geologic media (Thomsen, 1986).

For extrapolation, we require  $q_\alpha$  and  $q_\beta$  defined for media where  $\hat{p}$  and  $\hat{a}$  are not aligned. For P-waves, and in terms of  $q_{\alpha;i}$  and  $\alpha_i$  in the incident medium and  $q_{\alpha;r}$  and  $\alpha_r$  in the refracted medium, Snell's Law is invoked to get for P-waves to get

$$q_{\alpha;r}^2 = q_\alpha^2 + p_i^2 - p_1^2 - p_2^2, \quad (8)$$

with

$$q_{\beta_{sv};r}^2 = q_\alpha^2 + p_i^2 - p_1^2 - p_2^2, \quad (9)$$

for SV-waves and

$$q_{\beta_{SH};r}^2 = q_{\beta_{SH}}^2 + p_l^2 - p_1^2 - p_2^2, \quad (10)$$

for SH-waves.

For an incident planewave, equations 8, 9, and 10 determine vertical slowness for the planewave  $\varphi$  that refracts from  $z=0$  in the upper medium to  $z=\Delta z$  into the lower medium, where the following Fourier integral governs extrapolation (Gazdag, 1978)

$$\varphi_{\Delta z} = \varphi_0 e^{i\Delta z q \omega}. \quad (11)$$

Vertical slowness  $q$  can be any of equations 8, 9, and 10.

## Examples

To verify the performance of the operators described above, impulse responses for SV-waves in TTI media are generated. Figure 1a, b, c, and d demonstrates SV-wave propagation in a strong TI medium ( $\alpha_0=1991\text{ m/s}$ ,  $\beta_0=795\text{ m/s}$ ,  $\delta=0.161$ ,  $\varepsilon=-0.075$ ) where the elapsed time of wave propagation is 0.5 seconds. For Figures 1a and b, the axis of symmetry is normal to the surface (VTI). A slice through the SV wavefield at  $z = 0$  m shows a symmetric response as expected. A slice along X-line direction = 1250 m shows fast propagation in the In-line direction is fast (this is the fast direction), and it is slow in the vertical direction. Multi-arrivals are evident at ( $z = 1000$  m, In-line = 1600 m) and ( $z = 1000$  m, In-line = 3600 m). When this medium is 'tipped' to 45 degrees from normal, the  $z = 0$  m slice is now more complicated, and multi-arrivals are now apparent (compared to the VTI case in Figure 1a). The slice along X-line direction = 1250 m shows only one instance of multi-pathing ( $z = 1200$  m, In-line = 2500 m) and is clearly a rotated version of the VTI impulse in Figure 1b.

## Conclusions

Designed to reside at the centre of a phase shift algorithm for seismic imaging and modelling, a number of phase shift operators for transverse isotropy are detailed and implemented. Numerical examples are presented to demonstrate wavefront extrapolation for SV-waves. For a TI medium that is very strong, 3D impulse responses demonstrate the rather complex propagation paths followed by wave energy in what is a homogeneous medium. Significantly, multi-arrivals are apparent vertically in VTI media and vertically and in plane view for TTI media.

## Acknowledgements

Thanks to the sponsors of CREWES for their support of this work.

## References

- Bording, R. P., and Lines, L. R., 1997, Seismic modeling and imaging with the complete wave equation: Soc. of Expl. Geophys.
- Ferguson, R. J., and Sen, M. K., 2004, Estimation the elastic parameters of anisotropic media using a joint inversion of p-wave and sv-wave traveltimes error: Geophysical Prospecting, **52**, 547-558.
- Foster, D. J., and Mosher, C. C., 1992, Suppression of multiple reflections using the Radon transform: Geophysics, **57**, No. 03, 386-395.
- Foster, I., 1995, Designing and building parallel programs: Addison-Wesley.
- Kennett, B. L. N., 1983, Seismic wave propagation in stratified media: Cambridge University Press.
- Nichols, D. E., 1996, Maximum energy traveltimes calculated in the seismic frequency band: Geophysics, **61**, No. 01, 253-263.
- Thomsen, L., 1986, Weak elastic anisotropy: Geophysics, **51**, No. 10, 1954-1966, discussion in GEO-53-04-0558-0560 with reply by author.
- Udias, A., 1999, Principles of Seismology: Cambridge University Press.

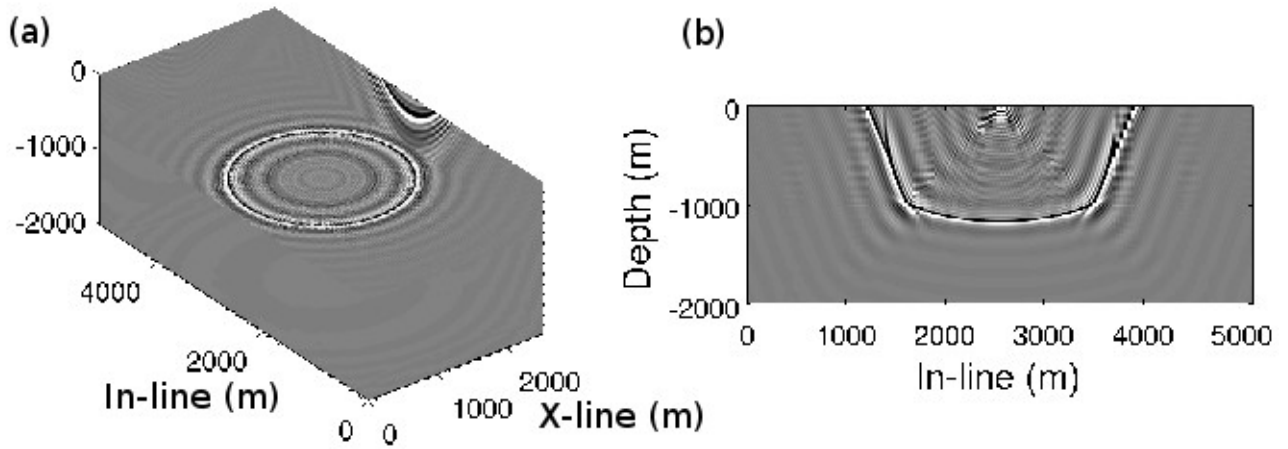


Figure 1: Impulse response for SV-waves in a VTI medium. a) A constant-depth slice. b) An in-line slice. Multi-arrivals are present at 1000 m depth and 1600 m and 3600 m in-line.

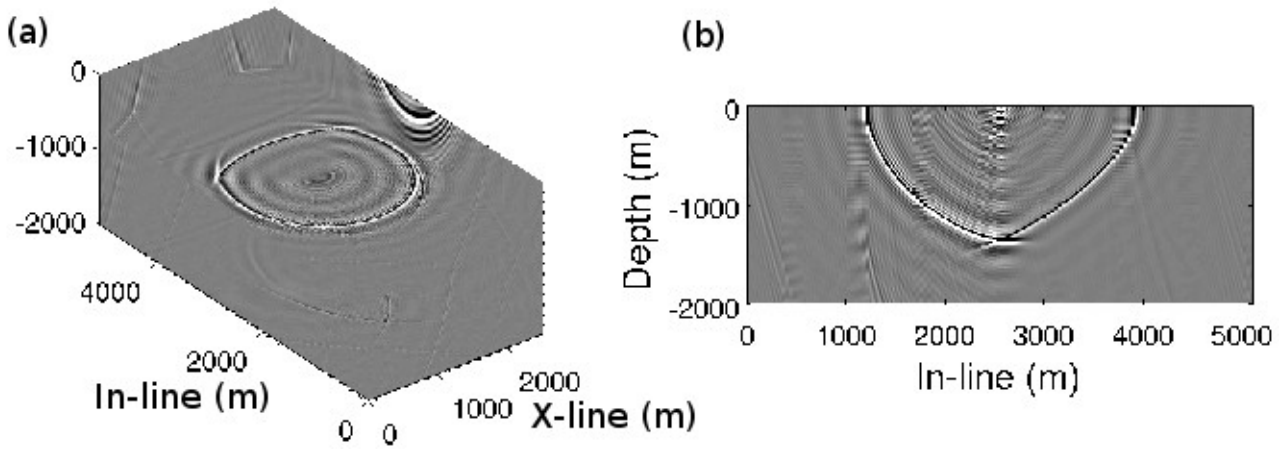


Figure 2: Impulse response for SV-waves in a TTI medium. a) A constant-depth slice. b) An in-line slice. Note multi-arrivals at 2550 m in-line and 1250 m depth.